

Theoretical Study of the Tautomerism in the One-Electron Oxidized Guanine–Cytosine Base Pair

J. P. Cerón-Carrasco* and A. Requena

Departamento de Química Física Facultad de Química, Universidad de Murcia, Campus de Espinardo, 30100 Murcia, Spain

E. A. Perpète[†] and C. Michaux[‡]

Unité de Chimie Physique Théorique et Structurale, Facultés Universitaires Notre-Dame de la Paix, Rue de Bruxelles, 61. 5000 Namur, Belgium

D. Jacquemin

CEISAM, UMR CNRS 6230, BP 92208, Université de Nantes, 2, Rue de la Houssinière, 44322 Nantes, Cedex 3, France

Received: February 25, 2010; Revised Manuscript Received: September 2, 2010

Ionizing radiation on DNA mainly generates one-electron oxidized guanine–cytosine base pair ($G^{+\bullet}:C$), and in the present paper we study all possible tautomers of $G^{+\bullet}:C$ by using *ab initio* approaches. Our calculations reveal that the tautomeric equilibrium follows a peculiar path, characterized by a stepwise mechanism: first the proton in the central hydrogen bond $N1(G)-H1-N3(C)$ migrates from guanine to cytosine, and then the cytosine cation releases one proton from its amino group. During this second step, water acts as a proton acceptor, localizing the positive charge on one of the water molecules interacting with the guanine radical. In agreement with experimental findings, the computed energy barriers show that the deprotonation of the cytosine cation is the speed-limiting step in the tautomeric equilibrium. The influence of the number of water molecules incorporated in the theoretical model is analyzed in detail. The evolution of electronic properties along the reaction path is also discussed on the basis of partial atomic charges and spin density distributions. This work demonstrates that water indeed plays a crucial role in the tautomeric equilibria of base pairs.

I. Introduction

DNA is constantly exposed to attacking environmental agents such as singlet oxygen, free radicals, or ionizing radiations; the resulting reactions finally give rise to alterations of the genetic code.^{1–9} In the case of ionizing radiations, the absorbed energy is high enough to remove an electron and to generate a radical cation (hole), which in an early stage could be localized on the DNA backbone, on the surrounding water molecules, or on one base pair.^{10,11} The hole generated during an ionization event can migrate through DNA by a hopping mechanism^{12–15} that can be interrupted by proton transfer between two bases on a given base pair, for example.^{16–20} Since guanine is the most oxidizable nucleic acid base in aqueous solution,¹⁷ the proton transfer mainly takes place in a one-electron oxidized guanine–cytosine base pair ($G^{+\bullet}:C$), and the interbase proton transfer in $G^{+\bullet}:C$ is the crucial step leading to the hole transfer and, indirectly, the DNA radiation damage mechanism.

In Figure 1 are shown the five possible paths for the proton transfer on the $G^{+\bullet}:C$ base pair:²¹ path A is the deprotonation of the $N1(G)$ -site giving the $G(-H1):C(H3)^+$ form; path B is the transfer of the $H2$ proton leading to the $G(-H2):C(H2)^+$ form; and path C is the removal of the $H2'$ proton from the amino group of the guanine to produce $G(-H2'):C$. The products resulting from paths A and B imply a protonated cytosine. By means of the pulse

radiolysis technique, Kobayashi and co-workers^{22,23} have reported experimental data which are consistent with path A followed by the release of one proton from the cytosine cation $C(H3)^+$ to solution. According to these recent measurements, the migration of the $H1$ proton in the $G^{+\bullet}:C$ base pair is a very fast reaction, as it involves the migration of a proton along one hydrogen bond.^{18,24,25} As a result, the rate constant of the whole reaction should be limited by the deprotonation of $C(H3)^+$. Nevertheless, to extend our study to the overall mechanism, the deprotonation of the $G^{+\bullet}:C$ base pair is also analyzed by considering the release of $H4'$ and $H1$ protons from the cytosine cation to solution, that is, paths D and E in Figure 1, respectively. It should be noted that in DNA duplexes the $N1$ atom of cytosine is covalently connected to the sugar unit through a $N-C$ bond. Subsequently, the deprotonation from $N1(C)-H1$ represented by path E does not take place in biological systems. We explore this alternative mechanism only to provide a comparison of the stability of all possible tautomers.

Though the molecular environment can strongly affect molecular geometries^{26–28} and the tautomeric equilibrium in the GC base pair, in both neutral^{29–35} and radical states,^{36–41} most of the previous theoretical studies addressing this problem have been carried out in the gas phase.^{19,42–44,7,45} As Ghosh and Schuster discussed,⁴⁶ when the surrounding environment is neglected in the model, calculations do predict that $G^{+\bullet}:C$ is the most stable structure,^{19,42–44} in disagreement with the experimental evidence of a spontaneous transfer of the $H1$ proton from the $N1$ of guanine to the cytosine $N3$ (path A) due to its relative acidity in the former position.^{16,47} We are only aware of a very recent paper by Kumar and Sevilla⁴⁸

* Corresponding author. E-mail: jpceron@um.es.

[†] Senior Research Associate of the Belgian FNRS.

[‡] Research Associate of the Belgian FNRS.

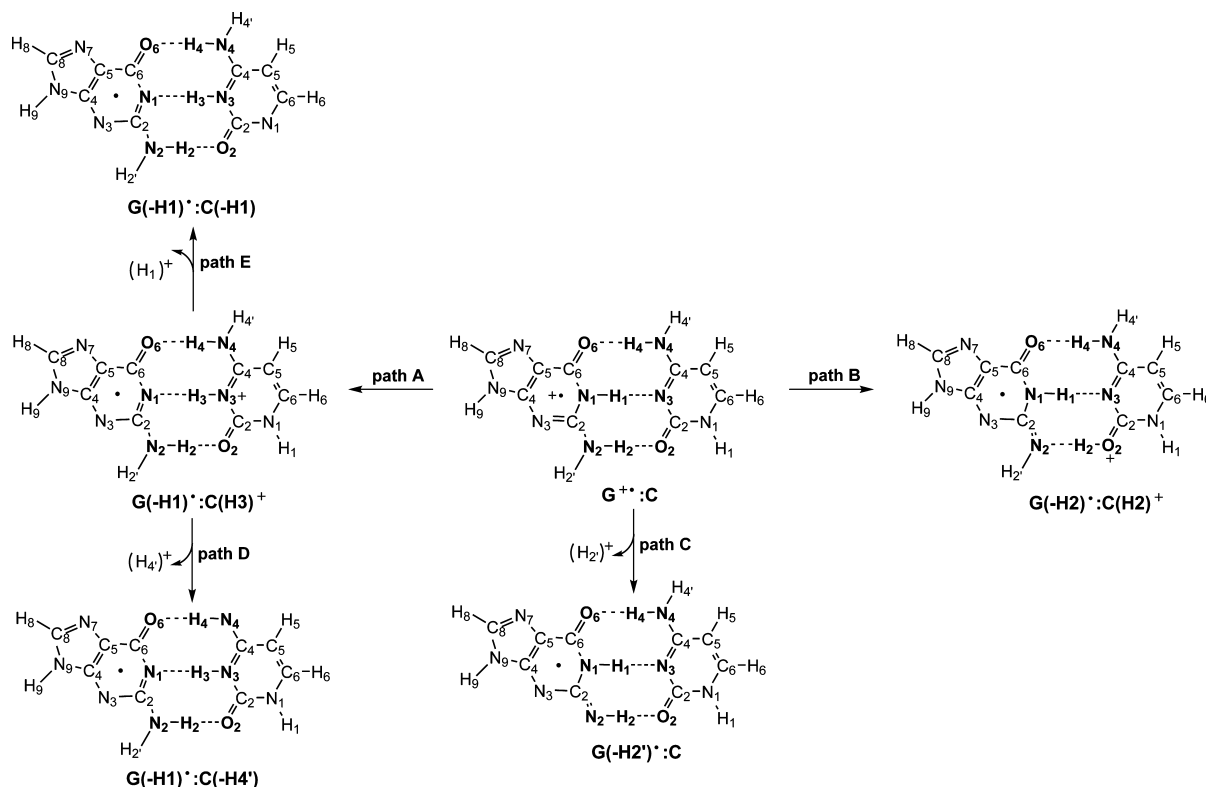


Figure 1. Possible proton transfer paths for the $G^{+}\cdots C$ base pair.

who considered the effect of the first hydration shell by explicit water molecules when modeling the H1 proton transfer in the $G^{+}\cdots C$ base pair. Their calculations indicate that this reaction is associated to a negative variation of Gibbs free energies⁴⁸ in contradiction with previous gas-phase computations and in agreement with experiment.^{22,23,49} Accordingly, it is crucial to consider solvated models, first because water molecules facilitate the proton transfer and second because they are obviously required to investigate the deprotonation of $C(H3)^{+}$.

To investigate the tautomerization of the one-electron oxidized guanine–cytosine base pair, we use in the present paper the methodology that allowed the successful study of the double proton transfer in neutral base pairs.^{50–52} To simulate the influence of the hydration which is a characteristic of the real biological environment, we have selected the two explicit solution models designed in our previous theoretical study devoted to neutral base pairs,⁵¹ with the six- and eleven-water-molecule systems shown in Figure 2. Consequently, we were also able to study the impact of the water molecules on each reaction step, and all possible paths (Figure 1) have been considered.

II. Theoretical Methods

All structures have been fully optimized without symmetry constraints using the BP86^{53,54} functional in connection with Pople's 6-311++G(d,p) basis set. This theoretical level is justified by its ability to provide accurate results for base pairs.^{26,27,50–52,55} The harmonic vibrational frequencies and thermodynamic corrections at 298 K were obtained at the same theoretical level. The vibrational analysis confirms the nature of stationary points: the absence of imaginary frequency for minima and a single imaginary mode for transition states (TS). The corresponding total energies of all the stationary points have been improved using the MP2/infinite basis set extrapolation developed by Truhlar,⁵⁶ which provides the most accurate results according to a recent benchmark investigation carried out for the GC base pair.⁵⁷ The basis set

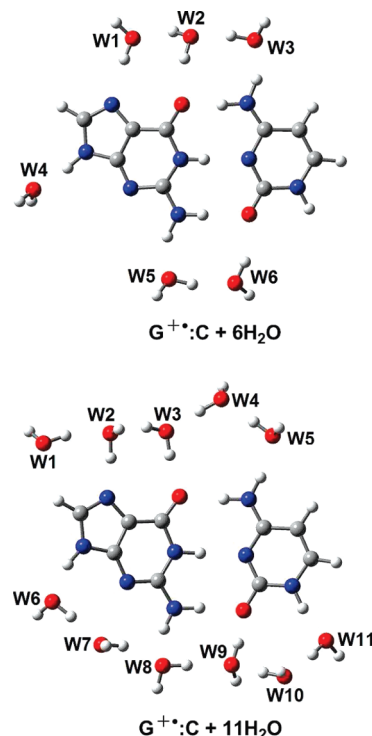


Figure 2. Geometries for solution models (see text). Carbon atoms are colored in gray, nitrogen in blue, and hydrogen in white.

extrapolation is based on a split of the total energy into its Hartree–Fock and correlation parts

$$E^{\text{tot}} = E^{\text{HF}} + E^{\text{cor}} \quad (1)$$

According to Truhlar's method, the basis-set limit for the total energy is calculated by the following equation

$$E_{\infty}^{\text{tot}} = \frac{3^{\alpha}}{3^{\alpha} - 2^{\alpha}} E_X^{\text{HF}} - \frac{2^{\alpha}}{3^{\alpha} - 2^{\alpha}} E_Y^{\text{HF}} + \frac{3^{\beta}}{3^{\beta} - 2^{\beta}} E_X^{\text{cor}} - \frac{2^{\beta}}{3^{\beta} - 2^{\beta}} E_Y^{\text{cor}} \quad (2)$$

where Y and X denote the cc-pVDZ and cc-pVTZ basis set levels, respectively, while α and β are fitting exponents. For the particular case of the MP2 method, these exponents are $\alpha = 3.4$ and $\beta = 2.2$. Partial atomic charges were evaluated using the Natural Bond Orbital (NBO) scheme.^{58–60} All our calculations were carried out with the Gaussian 03 package,⁶¹ while the analysis of the results was performed using GaussView.⁶²

III. Results and Discussions

Despite experimental evidence suggesting that in the $G^{+}\cdot:C$ base pair the migration of the H1 proton from guanine to cytosine results in the increase of the acidity at this position,^{49,63} we did not rule out any of the possible paths described in Figure 1. Thus, all tautomeric equilibria (paths A and B) as well as deprotonation mechanisms (paths C, D, and E) are investigated in Section A. In Section B we analyze the charges and spin density distributions for each optimized structure.

A. Optimized Geometries and Relative Energies. In physiological conditions, DNA base pairs undergo the influence of several environmental factors: stacking interactions, phosphate groups, surrounding water molecules, external cations, and the effects of other biological molecules. Among these different factors, we stress that the aqueous environment not only plays a major role in DNA's stability^{64,65} but also affects the geometry of the base pairs^{66,67} as well as their electronic structure.⁶⁸ Several approaches are available for the simulation of the aqueous solution: microhydrated structures,^{32,69,70} continuum solvent models,^{71,72} and large hydration schemes relying on hybrid quantum chemical/molecular dynamics methods.^{73–75} As a first approximation for the treatment of the solvent, X-ray crystal structures of DNA⁷⁶ are used here for the simulations of the first hydration shell through an explicit solvating model,⁷⁷ the experimental hydration sites being selected as starting points for theoretical calculations.^{69,76}

In our study, we have employed the six- and eleven-water-molecule microhydrated models shown in Figure 2. These two models were recently designed by Kumar et al. from the hydration pattern of base pairs imbedded in DNA, to study

microhydrated GC in the neutral and anionic radical states.^{48,78} In the six-water-molecule model, the surrounding water molecules are located around the N2(G), N3(G), O6(G), N7(G), O2(C), and N4(C) atoms (see numbering in Figure 1). In the larger eleven-water-molecule model, the five extra water molecules are added close to the remaining noncomplexed heteroatoms. These models are a suitable representation of the experimentally observed hydration shell of the GC base pair⁷⁶ and are also consistent with previous molecular dynamics simulations.^{79,80} Kumar et al. concluded that the six-water-molecule model is adequate to reproduce molecular dynamics results, though the calculated interbase hydrogen-bond distances are in better agreement with the X-ray data when the eleven-water-molecule model is applied (see ref 78 and references therein). Taking into account this previous evidence, we have adapted here both solution models to assess the tautomeric equilibrium and the linked deprotonation mechanism in a one-electron oxidized GC base pair. According to our calculations, when $G(-H2')\cdot:C(H2)^+$ (path B) or $G(-H2')\cdot:C$ (path C) geometries are used as starting points, the optimized geometry rapidly reverts to $G^{+}\cdot:C$, regardless of the solution model. To check the inaccessibility of both paths B and C, we have scanned the energy changes along N2(G)–H2 and N2(G)–H2' proton transfer (see Supporting Information for details), and these calculations confirm the absence of a stable product in both cases. Therefore, at this level of theory, the interbase proton transfer from the guanine cation to the cytosine is predicted to proceed solely through path A because $G(-H1)\cdot:C(H3)^+$ is the only product associated to a true energetic minimum.

On the other hand, the variations in energy associated with the migration of the H1 proton significantly depend on the number of water molecules surrounding the base pair. To clarify this point, the relative energies calculated with the six- and eleven-water-molecule models are listed in Table 1. As can be seen, the proton transfer process is not thermodynamically favored when six water molecules are taken into account. Indeed, from the total energy changes (ΔE), we found that under these conditions $G(-H1)\cdot:C(H3)^+$ is 1.84 kcal/mol less stable than the initial $G^{+}\cdot:C$ base pair, and this fact is reflected in the positive change of free energy. On the contrary, with the eleven-water-molecule model we obtain that the $G(-H1)\cdot:C(H3)^+$ total energy is 1.73 kcal/mol lower than its $G^{+}\cdot:C$ counterpart, with a negative free energy change, in agreement with experimental evidence.^{22,23,49} As we also show in Table 1, the calculated MP2 energy barrier heights for H1 proton transfer show trends similar

TABLE 1: Total Electronic Energy (E/au), Relative Energy ($\Delta E/\text{kcal mol}^{-1}$), and Relative Gibbs Free Energies at 298 K ($\Delta G/\text{kcal/mol}$) Calculated for the Tautomeric Equilibria in the Hydrated $G^{+}\cdot:C$ Base Pair^a

structure	MP2/infinite//BP86/6-311++G(d,p)			B3LYP/6-31+G(d,p)	
	E_{∞}^{tot}	ΔE	ΔG^b	ΔE^c	ΔG^c
six-water-molecule model					
$G^{+}\cdot:C$	−1394.419731	0.00	0.00	0.00	0.00
$[G(-H1)\cdot:C(H3)^+]^{\ddagger}$	−1394.414622	3.21	1.11	2.60	
$G(-H1)\cdot:C(H3)^+$	−1394.416791	1.84	1.92	0.93	0.90
$[G(-H1)\cdot:C(-H4')^{\ddagger}]^{\ddagger}$	−1394.400741	11.92	12.20		
$G(-H1)\cdot:C(-H4')$	−1394.402481	10.82	12.34		
eleven-water-molecule model					
$G^{+}\cdot:C$	−1776.370031	0.00 (0.00)	0.00 (0.00)	0.00	0.00
$[G(-H1)\cdot:C(H3)^+]^{\ddagger}$	−1776.365683	2.73	1.08	1.42	
$G(-H1)\cdot:C(H3)^+$	−1776.372785	−1.73 (−1.30)	−0.72 (−0.29)	−1.17	−0.65
$[G(-H1)\cdot:C(-H4')^{\ddagger}]^{\ddagger}$	−1776.351851	11.41	11.25		
$G(-H1)\cdot:C(-H4')$	−1776.353911	10.11 (13.41)	10.91 (14.20)		

^a Calculated PCM-MP2 energies for eleven-water-molecule models are given in parentheses. ^b Thermal corrections taken from unscaled vibrational calculations. ^c From ref 48.

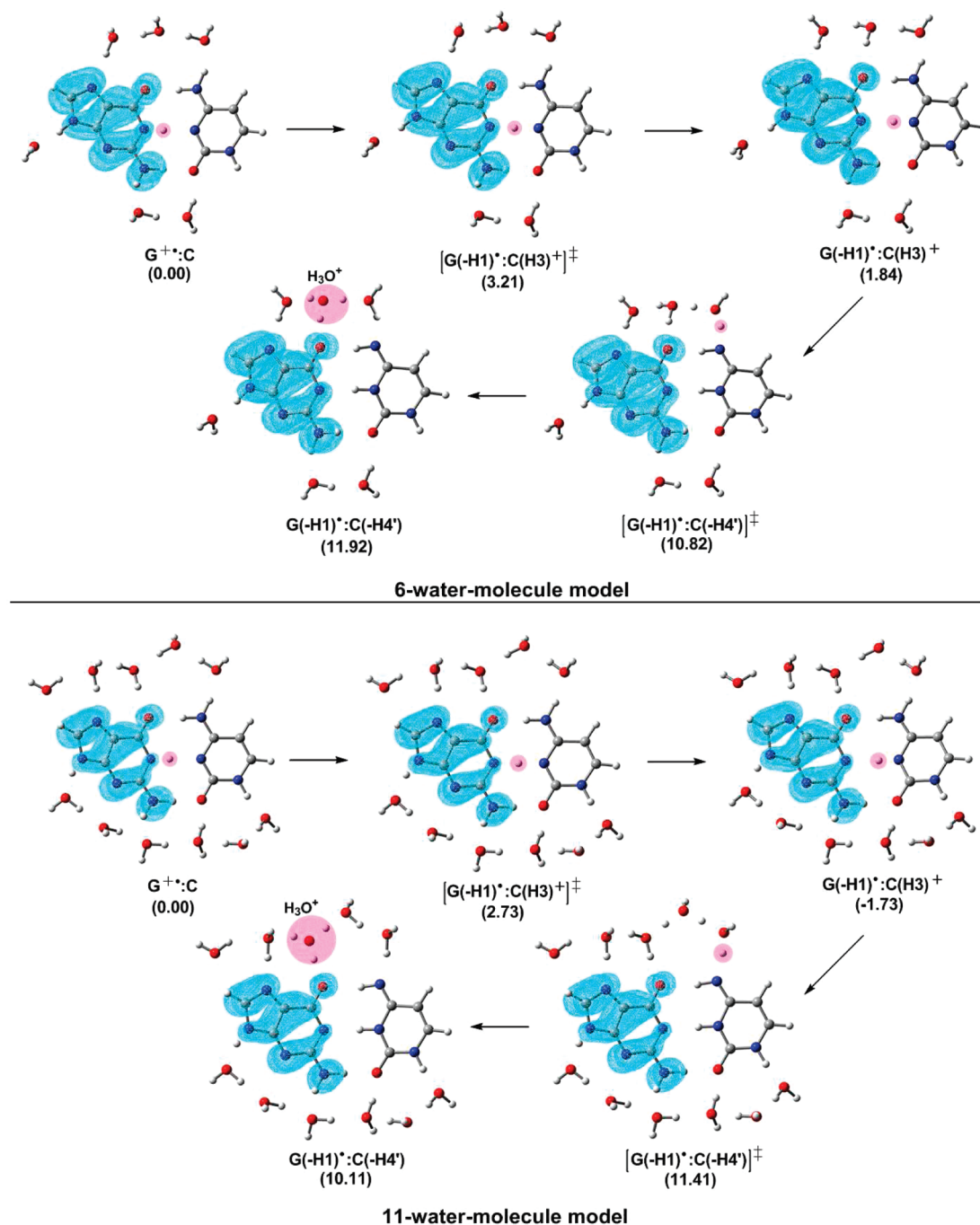


Figure 3. Optimized geometries along the proton transfer process onto the hydrated oxidized GC base pair. The values in parentheses are the relative total energies in kcal/mol, taking the canonical structure as reference. Unpaired spin density distribution for each optimized structure is also plotted. The pink circle highlights the transferred protons. For atom numbering, see Figure 1.

to previous B3LYP calculations,⁴⁸ results being in very good agreement for the variations of the free energy. As suggested by Kumar and Sevilla,⁴⁸ the discrepancies between the experimental and the smaller theoretical model are due to the fact that six water molecules only partially solvate the $G^{+\cdot}:C$ pair, whereas the system is fully solvated with eleven water molecules. These results agree with our previous study on neutral GC,⁵¹ where we demonstrated that the tautomeric equilibrium was significantly affected by the number of surrounding water molecules.

To extend our analysis, we determine the activation barrier energies along the reaction path connecting $G^{+\cdot}:C$ to $G(-H1)\cdot:C(H3)^+$ via the TS. The vibrational analysis shows that this TS is correctly characterized by only one imaginary frequency,

which is clearly related to the stretching of the H1 proton along the $N1(G)-H1-N3(C)$ bond, as expected. This imaginary frequency is 973i and 1026i cm^{-1} for six- and eleven-water-molecule models, respectively (for details, see the Supporting Information). Regarding the TS energies, it is proposed that proton transfers are subject to tunneling effect and thermal fluctuations,⁸¹ so that the activation barriers are only indicative. Nevertheless, it follows from the data presented in Table 1 that the H1 proton transfer is kinetically favored in the eleven-water-molecule model, due to a small energy difference between $[G(-H1)\cdot:C(H3)^+]^{\ddagger}$ and $G^{+\cdot}:C$.

Now that the H1 proton transfer process has been studied, we are able to investigate the release of a proton from $C(H3)^+$ to the solution, which apparently constitutes the only deproto-

nation accessible mechanism since neither path B nor C lead to stable structures. A glance at Figures 1 and 2 clearly hints at the only possibility that exists for the $C(H3)^+$ deprotonation if a six-water-molecule model is selected: that is, the $N4(C)-H4'$ proton transfer to the W3 water molecule (path D). On the other hand, for the eleven-water-molecule model, two paths can be followed: the $N4(C)-H4'$ proton transfer to the W5 water molecule (path D) or the $N1(C)-H1$ proton transfer to the W11 water molecule from the cytosine cation (path E). All these possible mechanisms have been investigated. As it was discussed before, since the $N1(C)$ site is bonded to the sugar ring in duplex DNA, path E is not realistic in biological systems, and it was included in our study for comparison purposes. Interestingly, it is possible to optimize the $G(-H1):C(-H1)$ structure, corresponding to another water-assisted mechanism through W9, W10, and W11 water molecules (see scan in Supporting Information). This finding does not affect our main conclusion, as only the $H4'$ deprotonation product is possible in the DNA duplex, but confirms the catalytic role played by water molecules in both intra- and interbase proton transfer mechanisms. The optimized final product for path D, $G(-H1):C(-H4')$, has been characterized to be much less stable than the intermediate $G(-H1):C(H3)^+$ (Table 1). These results can be explained as, in the first case, the positive charge is localized on a H_3O^+ , while in the latter the positive charge can be delocalized in the π system of cytosine (see also the next section). The comparison between $[G(-H1):C(H3)^+]^+$ and $[G(-H1):C(-H4')]^+$ energies allows us to conclude that the migration of the H1 proton in the first step is much faster than the deprotonation of the cytosine cation, and we are now able to offer a complete view of the deprotonation mechanism of G^+ in the solvated base pair. This picture is summarized in Figure 3 and indicates that the one-oxidized GC base pair is predicted to lead mainly to the $G(-H1):C(H3)^+$ structure.

It should be highlighted here that neither six- nor eleven-water-molecule models are large enough to fully solvate the protonated water molecule in the $G(-H1):C(-H4')$ structure because W2 and W3 stand at the border of our models. To estimate the possible error due to the size of the hydration shell, we have also carried out MP2 single-point calculations using the well-known polarizable continuum model (PCM) as implemented in Gaussian 03,⁶¹ considering water as the environment. Although compared to PCM-free calculations the general impact is a significant stabilization of all systems (an expected fact for a charged molecule), the relative total energies and free energies are not notably altered, though the energies of the $G(-H1):C(-H4')$ product are less stable by about 3 kcal/mol (Table 1). Furthermore, it is well-known that, in solution, H_3O^+ participates in three hydrogen bonds with surrounding water molecules.⁸² In our case, the H_3O^+ is not in a bulk water medium, but it is complexed to the guanine base: two of its protons are bound to two water molecules, and the third one is bound to the atom O6(G) (see Figure 3). Of course, the geometry obtained $G(-H1):C(-H4')$ is only a static picture of the final product. Indeed, in the real DNA environment, proton diffusion may occur through further water molecules. Though our study does not cover the proton diffusion in solution, in light of these results we can conclude that the eleven-water-molecule model is able to qualitatively simulate the experimental data for the one-electron oxidized GC base pair.

In the neutral GC base pair,⁵¹ no stable structure could be obtained for the first H1 proton transfer. In contrast, for the radical cation state, not only is it possible to optimize the $G(-H1):C(H3)^+$ minimum but also this structure is the most

TABLE 2: Changes in Spin Distribution ($|\ell|$) with Proton Transfer

atom	$G^+:C$	$G(-H1):C(H3)^+$	$G(-H1):C(-H4')$
six-water-molecule model			
N2	0.227402	0.225499	0.263895
N3	0.268582	0.276536	0.283747
C5	0.257520	0.275908	0.265078
C8	0.216959	0.220306	0.201859
eleven-water-molecule model			
N2	0.211639	0.188841	0.220977
N3	0.233579	0.252188	0.264798
C5	0.235403	0.267078	0.280045
C8	0.197414	0.208908	0.190545

stable (see Table 1). This essential dissimilarity is in total agreement with the experimental data suggesting that the enhanced acidity of the H1 proton in the one-electron oxidized GC base pair indeed activates the deprotonation from this site.^{16,47} On the other hand, for both neutral and radical cation base pairs, water molecules do not act as passive elements and play a crucial role: (i) in the case of the neutral GC base pair, tautomeric equilibrium must be assisted by surrounding water molecules,⁵¹ leading to the double proton transfer product, and (ii) for the one-electron oxidized base, the release of proton from $C(H3)^+$ giving the deprotonated base pair requires the participation of the nearby solvent molecules.

B. Spin Density and Charge Distribution. Aiming at understanding and describing the electronic changes implied by the tautomeric equilibrium, we have also studied the proton transfer effects on the spin densities and on the charge distributions. Experimentally, combinations of electron paramagnetic resonance (EPR) and electron–nuclear double resonance (ENDOR) methods have been extensively used by Close, Nelson, and their co-workers^{83–89} for studying the structure and the nature of radicals in DNA constituents. According to these EPR and ENDOR studies, the single unpaired electron is localized on the guanine base after irradiation. The calculated spin density of Figure 3 confirms that the radical is confined on the guanine base during the H1 proton transfer, as it was recently proposed by Kumar and Sevilla,⁴⁸ and this also holds for the cytosine cation deprotonation reaction. To get additional insights about the effect of proton transfer on the radical localization, Table 2 lists atomic spin densities for selected guanine atoms (see Supporting Information for the complete data). It is clear from Table 2 that the radical is mainly centered around four atoms: N2, N3, C5, and C8 of guanine. Furthermore, it can be seen that the calculated values for spin densities remain practically unchanged upon proton transfer. Let us emphasize: the spin distribution in the guanine base is not affected by the proton transfer related to the tautomeric equilibrium.

In addition, we have also studied the partial atomic charges through the NBO scheme. As shown in Table 3, both six- and eleven-water-molecule models show similar trends for charge distribution during the proton transfer (see Supporting Information for complete data): the positive charge in the canonical structure $G^+:C$ is mainly localized on the guanine base (+0.765 $|\ell|$ and +0.725 $|\ell|$ for the six- and the eleven-water-molecule models, respectively), while the cytosine base and the surrounding water molecules remain almost neutral. When the H1 proton is transferred, the deprotonation product $G(-H1):C(H3)^+$ is obtained, in which the cytosine has the positive charge (+0.794 $|\ell|$ and +0.763 $|\ell|$ for six-water- and eleven-water-molecule models, respectively), with no significant participation of surrounding water molecules. From the values included in Table 3, we can also state that solvent effects on the charge

TABLE 3: Changes in Molecular Charges (|e|) with Proton Transfer

	$G^{+•}:C$	$G(-H1)^•:C(H3)^+$	$G(-H1)^•:C(-H4')$
six-water-molecule model			
guanine (G)	0.765	0.086	0.078
cytosine (C)	0.122	0.794	0.066
water 2 (W2)	0.003	0.021	0.676
eleven-water-molecule model			
guanine (G)	0.725	0.077	0.073
cytosine (C)	0.129	0.763	0.062
water 3 (W3)	0.014	0.015	0.659

distribution are negligible in this first step. However, our results show the crucial role of water molecules acting as a proton acceptor in the subsequent deprotonation of the cytosine cation $C(H3)^+$.

Notably, the optimized structures for $G(-H1)^•:C(-H4')$ in solution (see Figure 3) indicate that the $H4'$ proton is not trapped by the closest water molecule, that is, W3 and W5 in six- and eleven-water-molecule models, respectively. Indeed, the $H4'$ release to solution goes from $C(H3)^+$ to W2 in the first model, while W3 is concerned in the second one, via the assisted-water proton transfer (see NBO charges in Table 3). This issue is corroborated by the analysis of the TS connecting $G(-H1)^•:C(H3)^+$ to $G(-H1)^•:C(-H4')$, as its characteristic imaginary frequency is associated to the simultaneous stretching of the $N4-H4'$ bond and of all the water bonds involved in the assisted proton transfer (the calculated values are 269i and 211i cm^{-1} for $[G(-H1)^•:C(-H4')]^{\ddagger}-6H_2O$ and $[G(-H1)^•:C(-H4')]^{\ddagger}-11H_2O$, respectively). We would like to point out that this water-assisted phenomenon is parallel to the mechanism observed for the double proton transfer in the neutral GC base pair. This result backs up the importance of including explicit solvent models in the study of tautomeric equilibria between base pairs in both their neutral and radical states.

IV. Conclusions

The tautomerism mechanisms in the one-electron oxidized guanine–cytosine base pair have been studied by MP2/infinite//BP86/6-311++G(d,p) calculations. Two solvated models were considered by analyzing the optimized geometries, vibrational frequencies, and relative energies, and it is shown that deprotonation of $G^{+•}:C$ through H1 proton transfer is the thermodynamically favored mechanism in solution, i.e., when the base pair is fully hydrated. Using the same theoretical level, our calculations show that $G(-H1)^•:C(-H4')$ is the most likely product for the deprotonation of the cytosine cation via water-assisted transfer. Therefore, the tautomeric equilibrium follows a stepwise mechanism: the H1 proton is first transferred, giving rise to the $G(-H1)^•:C(H3)^+$ intermediate, whereas in the second step, the water-assisted transfer of the $H4'$ proton provides the final product. From relative transition state energies, we have also confirmed that the first step is associated to a fast reaction, whereas the second step could be considered as the speed-limiting component, in good agreement with available experimental evidence. Of course, a more accurate simulation of the tautomerism in the oxidized GC base pair in DNA would require a more complex model for biological environment. In that framework, our results clearly indicate the active role played by water molecules on deprotonation mechanism and hint that the radiation-induced DNA damage could also be influenced by catalytic water molecules. Such investigation is carried out by our group.

Acknowledgment. The work was partially supported by the Ministerio de Educación y Ciencia of Spain under Project CTQ2007-66528 and by the Fundación Séneca del Centro de Coordinación de la Investigación de la Región de Murcia under Project 08735/PI/08. J.P.C.—C. acknowledges a research grant provided by the Fundación Cultural Esteban Romero, Obra Social CajaMurcia. E.A.P. and C.M. thank the Belgian National Fund for Scientific Research for their respective positions. Most of the calculations have been performed on the Servicio de Apoyo a la Investigación Tecnológica (SEDIC-SAIT), at the Universidad Politécnica de Cartagena (Spain), and on the Interuniversity Scientific Computing Facility (ISCF), installed at the Facultés Universitaires Notre-Dame de la Paix (Namur, Belgium), for which the authors gratefully acknowledge the financial support of the FNRS-FRFC and the “Loterie Nationale” for the convention number 2.4578.02 and of the FUNDP.

Supporting Information Available: Figures showing total energy changes along paths B, C, and E; the complete list of atomic spin distribution and charges; visualization of the normal modes with the imaginary frequency for transitions states. This material is available free of charge via the Internet at <http://pubs.acs.org>.

References and Notes

- (1) Bensasson, R. V.; Land, E. J.; Truscott, T. G. *Excited States and free Radicals in Biology and Medicine*; Oxford University Press: Oxford, 1993.
- (2) Burrows, C. J.; Muller, J. G. *Chem. Rev.* **1998**, *98*, 1109–1151.
- (3) Šponer, J.; Lankaš, F., Eds. *Computational Studies of RNA and DNA*; Springer: Dordrecht, The Netherlands, 2006; pp 419–421.
- (4) Jena, N. R.; Mishra, P. C.; Suhai, S. *J. Phys. Chem. B* **2009**, *113*, 5633–5644.
- (5) Kumar, A.; Sevilla, M. D. *J. Phys. Chem. B* **2009**, *113*, 13374–13380.
- (6) Kumar, A.; Sevilla, M. D. *Chem. Rev.* doi 10.1021/cr100023g.
- (7) Cauët, E.; Dehareng, D.; Liévin, J. *J. Phys. Chem. A* **2006**, *110*, 9200–9211.
- (8) Cauët, E.; Liévin, J. *J. Phys. Chem. A* **2009**, *113*, 9881–9890.
- (9) Cauët, E.; Valiev, M.; Weare, J. H. *J. Phys. Chem. B* **2010**, *114*, 5886–5894.
- (10) Jaeger, H. M.; Schaffer-III, H. F. *J. Phys. Chem. B* **2009**, *113*, 8142–8148.
- (11) Lee, Y. A.; Durandin, A.; Dedon, P. C.; Geacintov, N. E.; Shafirovich, V. *J. Phys. Chem. B* **2008**, *112*, 1834–1844.
- (12) Berlin, Y. A.; Burin, A.; Ratner, M. A. *J. Chem. Phys. A* **2000**, *104*, 443–445.
- (13) Lewis, F. D.; Letsinger, R. L.; Wasielewski, M. R. *Acc. Chem. Res.* **2001**, *34*, 159–170.
- (14) Takada, T.; Kawai, K.; Fujitsuka, M.; Majima, T. *Proc. Natl. Acad. Sci. U.S.A.* **2004**, *101*, 14002–14006.
- (15) O'Neill, M. A.; Barton, J. K. *J. Am. Chem. Phys.* **2004**, *126*, 11471–11483.
- (16) Steenken, S. *Chem. Rev.* **1989**, *89*, 503–520.
- (17) Steenken, S.; Jovanovic, S. V. *J. Am. Chem. Soc.* **1997**, *119*, 617–618.
- (18) Steenken, S. *Biol. Chem.* **1997**, *378*, 1293–1297.
- (19) Hutter, M.; Clark, T. *J. Am. Chem. Soc.* **1996**, *118*, 7574–7577.
- (20) Liu, C.-S.; Hernandez, R.; Schuster, G. *J. Am. Chem. Soc.* **2004**, *126*, 2877–2884.
- (21) Chatgililoglu, C.; Caminal, C.; Altieri, A.; Vougioukalakis, G. C.; Mulazzani, Q. G.; Gimisis, T.; Guerra, M. *J. Am. Chem. Soc.* **2006**, *128*, 13796–13805.
- (22) Kobayashi, K.; Tagawa, S. *J. Am. Chem. Soc.* **2003**, *125*, 10213–10218.
- (23) Kobayashi, K.; Yamagami, R.; Tagawa, S. *J. Phys. Chem. B* **2008**, *112*, 10752–10757.
- (24) Douhal, A.; Kim, S. K.; Zewail, A. H. *Nature* **1995**, *378*, 260–263.
- (25) Zewail, A. H. *J. Phys. Chem.* **1996**, *100*, 12701–12724.
- (26) Guerra, C. F.; Bickelhaupt, F.; Snijders, J.; Baerends, E. *J. Am. Chem. Soc.* **2000**, *122*, 4117–4128.
- (27) van der Wijst, T.; Guerra, C. F.; Swart, M.; Bickelhaupt, F. *Chem. Phys. Lett.* **2006**, *426*, 415–421.
- (28) Li, D.; Ai, H. *J. Phys. Chem. B* **2009**, *113*, 11732–11742.

- (29) Gorb, L.; Leszczynski, J. *J. Am. Chem. Soc.* **1998**, *120*, 5024–5032.
- (30) Alemán, C. *Chem. Phys.* **1999**, *244*, 151–162.
- (31) Alemán, C. *Chem. Phys.* **2000**, *253*, 13–19.
- (32) Shishkin, O. V.; Gorb, L.; Leszczynski, J. *J. Phys. Chem. B* **2000**, *104*, 5357–5361.
- (33) Podolyan, Y.; Gorb, L.; Leszczynski, J. *Int. J. Mol. Sci.* **2003**, *4*, 410–421.
- (34) Gorb, L.; Podolyan, Y.; Dziekonski, P.; Sokalski, W. A.; Leszczynski, J. *J. Am. Chem. Soc.* **2004**, *126*, 10119–10129.
- (35) Kabelac, M.; Hobza, P. *Phys. Chem. Chem. Phys.* **2007**, *9*, 903–917.
- (36) Shafirovich, V.; Cadet, J.; Gasparutto, D.; Dourandin, A.; Huang, W.; Geacintov, N. E. *J. Chem. Phys. B* **2001**, *105*, 586–592.
- (37) Gervasio, F. L.; Laio, A.; Iannuzzi, M.; Parrinello, M. *Chem.—Eur. J.* **2004**, *10*, 4846–4852.
- (38) Anderson, R. F.; Shinde, S. S.; Maroz, A. *J. Am. Chem. Soc.* **2006**, *128*, 15966–15967.
- (39) Chen, H.-Y.; Kao, C.-L.; Hsu, S. *J. Am. Chem. Soc.* **2009**, *131*, 15930–15938.
- (40) Agnihotri, N.; Mishra, P. C. *J. Phys. Chem. B* **2009**, *113*, 3129–3138.
- (41) Agnihotri, N.; Mishra, P. C. *J. Phys. Chem. B* **2010**, *114*, 7391–7404.
- (42) Colson, A. O.; Besler, B.; Sevilla, M. D. *J. Phys. Chem.* **1992**, *96*, 9787–9794.
- (43) Bertran, J.; Oliva, A.; Rodríguez-Santiago, L.; Sodupe, M. *J. Am. Chem. Soc.* **1998**, *120*, 8159–8176.
- (44) Li, X.; Cai, Z.; Sevilla, M. D. *J. Phys. Chem. B* **2001**, *105*, 10115–10123.
- (45) Rak, J.; Makowska, J.; Voityuk, A. A. *Chem. Phys.* **2006**, *325*, 567–574.
- (46) Ghosh, A. K.; Schuster, G. B. *J. Am. Chem. Soc.* **2006**, *128*, 4172–4173.
- (47) Candeias, L. P.; Steenken, S. *J. Am. Chem. Soc.* **1992**, *114*, 699–704.
- (48) Kumar, A.; Sevilla, M. D. *J. Phys. Chem. B* **2009**, *113*, 11359–11361.
- (49) Adhikary, A.; Khanduri, D.; Sevilla, M. D. *J. Am. Chem. Soc.* **2009**, *131*, 8614–8619.
- (50) Cerón-Carrasco, J. P.; Requena, A.; Michaux, C.; Perpète, E. A.; Jacquemin, D. *J. Phys. Chem. A* **2009**, *113*, 7892–7898.
- (51) Cerón-Carrasco, J. P.; Requena, A.; Zúñiga, J.; Michaux, C.; Perpète, E. A.; Jacquemin, D. *J. Phys. Chem. A* **2009**, *113*, 10549–10556.
- (52) Cerón-Carrasco, J. P.; Requena, A.; Perpète, E. A.; Michaux, C.; Jacquemin, D. *Chem. Phys. Lett.* **2009**, *484*, 64–68.
- (53) Becke, A. J. *Chem. Phys.* **1993**, *98*, 5648–5652.
- (54) Perdew, J. *Phys. Rev. B* **1986**, *33*, 8822–8824.
- (55) Swart, M.; Fonseca-Guerra, C.; Bickelhaupt, F. M. *J. Am. Chem. Soc.* **2004**, *126*, 16718–16719.
- (56) Truhlar, D. G. *Chem. Phys. Lett.* **1998**, *294*, 45–48.
- (57) Sponer, J.; Jurecka, P.; Hobza, P. *J. Am. Chem. Soc.* **2004**, *126*, 10142–10151.
- (58) Foster, J. P.; Weinhold, F. *J. Am. Chem. Soc.* **1980**, *102*, 7211–7218.
- (59) Reed, A. E.; Weinstock, R. B.; Weinhold, F. *J. Chem. Phys.* **1985**, *83*, 735–746.
- (60) Carpenter, J. F.; Weinhold, F. *J. Mol. Struct. (Theochem)* **1988**, *169*, 41–62.
- (61) Frisch, M. J.; Trucks, G. W.; Schlegel, H. B.; Scuseria, G. E.; Robb, M. A.; Cheeseman, J. R.; Montgomery, J. A., Jr.; Vreven, T.; Kudin, K. N.; Burant, J. C.; Millam, J. M.; Iyengar, S. S.; Tomasi, J.; Barone, V.; Mennucci, B.; Cossi, M.; Scalmani, G.; Rega, N.; Petersson, G. A.; Nakatsuji, H.; Hada, M.; Ehara, M.; Toyota, K.; Fukuda, R.; Hasegawa, J.; Ishida, M.; Nakajima, T.; Honda, Y.; Kitao, O.; Nakai, H.; Klene, M.; Li, X.; Knox, J. E.; Hratchian, H. P.; Cross, J. B.; Bakken, V.; Adamo, C.; Jaramillo, J.; Gomperts, R.; Stratmann, R. E.; Yazyev, O.; Austin, A. J.; Cammi, R.; Pomelli, C.; Ochterski, J. W.; Ayala, P. Y.; Morokuma, K.; Voth, G. A.; Salvador, P.; Dannenberg, J. J.; Zakrzewski, V. G.; Dapprich, S.; Daniels, A. D.; Strain, M. C.; Farkas, O.; Malick, D. K.; Rabuck, A. D.; Raghavachari, K.; Foresman, J. B.; Ortiz, J. V.; Cui, Q.; Baboul, A. G.; Clifford, S.; Cioslowski, J.; Stefanov, B. B.; Liu, G.; Liashenko, A.; Piskorz, P.; Komaromi, I.; Martin, R. L.; Fox, D. J.; Keith, T.; Al-Laham, M. A.; Peng, C. Y.; Nanayakkara, A.; Challacombe, M.; Gill, P. M. W.; Johnson, B.; Chen, W.; Wong, M. W.; Gonzalez, C.; Pople, J. A. *Gaussian 03*, revision C.02; Gaussian, Inc.: Wallingford, CT, 2004.
- (62) Dennington, R., II; Keith, T.; Millam, J.; Eppinnett, K.; Hovell, W. L.; Gilliland, R.; *GaussView*, Version 3.09, Semichem, Inc.: Shawnee Mission, KS, 2003.
- (63) Candeias, L. P.; Steenken, S. *J. Am. Chem. Soc.* **1989**, *111*, 1094–1099.
- (64) Rueda, M.; Kalko, S. G.; Luque, F. J.; Orozco, M. *J. Am. Chem. Soc.* **2003**, *125*, 8007–8014.
- (65) Rueda, M.; Kalko, S. G.; Luque, F. J.; Orozco, M. *J. Am. Chem. Soc.* **2006**, *128*, 3608–3619.
- (66) Zhanpeisov, N. U.; Leszczynski, J. *J. Phys. Chem. A* **1998**, *102*, 6167–6172.
- (67) Zhanpeisov, N. U.; Leszczynski, J. *J. Mol. Struct. (Theochem)* **1999**, *487*, 107–115.
- (68) Slavíček, P.; Winter, B.; Faubel, M.; Bradforth, S. E.; Jungwirth, P. *J. Am. Chem. Soc.* **2009**, *131*, 6460–6467.
- (69) Kumar, A.; Mishra, P. C.; Suhai, S. *J. Phys. Chem. A* **2005**, *109*, 3971–3979.
- (70) Park, H. S.; Nam, S. H.; Song, J. K.; Park, S. M.; Ryu, S. *J. Phys. Chem. A* **2008**, *112*, 9023–9030.
- (71) Herbert, H. E.; Halls, M. D.; Hratchian, H. P.; Raghavachari, K. *J. Phys. Chem. B* **2006**, *110*, 3336–3343.
- (72) Pacureanu, L.; Simon, Z. *Int. J. Quantum Chem.* **2010**, *110*, 1295–1305.
- (73) Jagoda-Cwiklik, B.; Slavíček, P.; Cwiklik, L.; Nolting, D.; Winter, B.; Jungwirth, P. *J. Phys. Chem. A* **2008**, *112*, 3499–3505.
- (74) Roca-Sanjuán, D.; Olaso-González, G.; Rubio, M.; Coto, P. B.; Merchán, M.; Ferré, N.; Ludwig, V.; Serrano-Andrés, L. *Pure Appl. Chem.* **2009**, *81*, 743–754.
- (75) Zhao, Z.; Rogers, D. M.; Beck, T. L. *J. Chem. Phys.* **2010**, *132*, 014502.
- (76) Schneider, B.; Berman, H. M. *Biophys.* **1995**, *69*, 2661–2669.
- (77) Moroni, F.; Famulari, A.; Raimondi, M. *J. Phys. Chem. A* **2001**, *105*, 1169–1174.
- (78) Kumar, A.; Sevilla, M. D.; Suhai, S. *J. Phys. Chem. B* **2008**, *112*, 5189–5198.
- (79) Auffinger, P.; Westhof, E. *J. Mol. Biol.* **2000**, *300*, 1113–1131.
- (80) Makarov, V.; Pettitt, B. M.; Feig, M. *Acc. Chem. Res.* **2002**, *35*, 376–384.
- (81) Miura, S.; Tuckerman, M. E.; Klein, M. L. *J. Chem. Phys.* **1998**, *109*, 5290–5299.
- (82) Marx, D.; Tuckerman, M. E.; Hutter, J.; Parinello, M. *Nature* **1999**, *397*, 601–604.
- (83) Jayatilaka, N.; Nelson, W. H. *J. Phys. Chem. B* **2007**, *111*, 800–810.
- (84) Jayatilaka, N.; Nelson, W. H. *J. Phys. Chem. B* **2007**, *111*, 7887–7896.
- (85) Close, D. M. *Radiat. Res.* **1993**, *135*, 1–15.
- (86) Close, D. M.; Nelson, W. H.; Sagstuen, E.; Hole, E. O. *Free Radical Res. Commun.* **1989**, *6*, 83–85.
- (87) Sagstuen, E.; Hole, E. O.; Nelson, W. H.; Close, D. M. *Free Radical Res. Commun.* **1989**, *6*, 91–92.
- (88) Hole, E. O.; Sagstuen, E.; Nelson, W. H.; Close, D. M. *Free Radical Res. Commun.* **1989**, *6*, 87–90.
- (89) Hole, E. O.; Nelson, W. H.; Close, D. M.; Sagstuen, E. *J. Chem. Phys.* **1987**, *86*, 5218–5219.